

Violation of hyperbolicity in a diffusive medium with local hyperbolic attractor

Pavel V. Kuptsov*

Department of Informatics, Saratov State Law Academy, Volskaya 1, Saratov 410056, Russia

Sergey P. Kuznetsov

*Kotel'nikov Institute of Radio Engineering and Electronics of RAS,
Saratov Branch, Zelenaya 38, Saratov 410019, Russia*

(Dated: May 29, 2019)

Departing from a system of two non-autonomous amplitude equations, demonstrating hyperbolic dynamics, we construct a 1D medium as ensemble of such local elements introducing spatial coupling via diffusion. When the length of the medium is small, all spatial cells oscillate synchronously, reproducing the local hyperbolic dynamics. This regime is characterized by a single positive Lyapunov exponent. The hyperbolicity survives when the system gets larger in length so that the second Lyapunov exponent passes zero, and the oscillations become inhomogeneous in space. However, at a point where the third Lyapunov exponent becomes positive, some bifurcation takes place that results in violation of the hyperbolicity. Beyond of this transition point, the system demonstrates an extensive spatiotemporal chaos typical for extended chaotic systems: the Kaplan-Yorke dimension, the number of positive Lyapunov exponents and the upper estimate for Kolmogorov-Sinai entropy grow linearly with the length of the system, while the Lyapunov spectrum tends to a limiting curve as the length grows.

PACS numbers: 05.45.-a, 05.45.Jn, 47.27.Cn

Keywords: hyperbolic attractor; high-dimensional chaos; Lyapunov exponents; covariant Lyapunov vectors; verification of hyperbolicity; Ginzburg-Landau equations

Introduction

One of the central concepts in mathematical theory of dynamical systems relates to hyperbolic strange attractors. Tangent space of each point of such an attractor splits into expanding and contracting subspaces, and this splitting is invariant. Dynamics on a hyperbolic attractor is structurally stable, i.e. is insensible to variations of parameters. It manifests strong stochastic properties and allows detailed theoretical analysis [1, 2].

During the last 40 years hyperbolic attractors were considered rather as idealized model of perfect chaos. Though some artificial systems with hyperbolic attractors were known, they were useless for practical applications because of complicated construction. Recently, a realistic system was suggested and implemented as electronic device, dynamics of which in stroboscopic description is associated with attractor of Smale-Williams type [3, 4]. Attractor of this system is hyperbolic as proven numerically by a method of verification of the cone criterion [5]. In paper [6] the amplitude equation for this system was studied, and the hyperbolicity was also proven by the method of cones. (Some other models based on the same principle are considered in Refs. [7, 8, 9, 10].)

Traditionally, studies of hyperbolic dynamics are mostly concentrated on finite dimensional systems. Many topics concerning spatiotemporal chaos, though attracted a lot of interest, remain open [11]. In this paper

we address a problem of survival of hyperbolicity of a spatiotemporal system when the length of the system grows. We consider a 1D extended system composed of local elements possessing a hyperbolic attractor that is based on the amplitude equations from [6]. The spatial coupling is introduced via diffusion. In fact, a system we study is a set of two coupled non-autonomous Ginzburg-Landau equations of special form.

We are aware of two numerical methods for reliable verification of hyperbolicity. The first one is the method based on the cone criterion [5], which employs directly the rigorous theorem, and, hence, looks preferable. Unfortunately, the method is appropriate only for low dimensional systems, while its extension to systems of many degrees of freedom seems to be abundantly sophisticated. The second method is based on a recently suggested routine of computing of covariant Lyapunov vectors [12]. These vectors are associated with Lyapunov exponents and indicate directions of stable and unstable manifolds at each point of an attractor. If these vectors are known, angles between each stable and each unstable direction can be computed and the minimal one can be found. The attractor is interpreted as non-hyperbolic, if the distribution of these angles does not vanish at the origin. In fact, this is only a sufficient condition because the converse is not true. In the present paper we develop and apply more subtle approach that allows to detect a tangency of two arbitrary vectors from stable and unstable subspaces.

The paper is organized as follows. In Sec. I we introduce the system and briefly discuss its local dynamics. Also we describe a numerical method applied to find solutions for the system. Sec. II represents linear stability analysis. The critical length of the system is determined

*Corresponding author. Electronic address: p.kuptsov@rambler.ru

where a spatially homogeneous solution becomes unstable with respect to non-uniform perturbation. Sec. III is devoted to illustrations of spatiotemporal dynamics. Sec. IV is the main part of the paper, where the Lyapunov analysis for the system is developed. We discuss distributions of minimal angles between vectors in stable and unstable tangent subspaces on the attractor. Also, dependencies of Lyapunov exponents, Kaplan-Yorke dimension and Kolmogorov-Sinai entropy on the length of the system are considered. In Sec. V we summarize the obtained results and outline perspectives for further investigations.

I. THE MODEL AND NUMERICAL METHOD

Let us start with amplitude equations for a physical model, demonstrating hyperbolic dynamics, suggested by Kuznetsov in Ref. [3]. It consists of two coupled non-autonomous van der Pol oscillators that are parametrically influenced by an external periodic force. The oscillators become active turn by turn, and pass the excitation each other in such way that the phase of oscillations is doubled after each period of the forcing. The amplitude equations for this system read [6]:

$$\begin{aligned}\dot{a} &= A \cos(2\pi t/T)a - |a|^2 a - i\epsilon b, \\ \dot{b} &= -A \cos(2\pi t/T)b - |b|^2 b - i\epsilon a^2.\end{aligned}\quad (1)$$

In this paper we study a spatially extended analog of this model, supplying it with the second spatial derivatives.

So, we consider two coupled non-autonomous Ginzburg-Landau equations:

$$\begin{aligned}\partial_t a &= A \cos(2\pi t/T)a - |a|^2 a - i\epsilon b + \partial_x^2 a, \\ \partial_t b &= -A \cos(2\pi t/T)b - |b|^2 b - i\epsilon a^2 + \partial_x^2 b.\end{aligned}\quad (2)$$

Here $a \equiv a(x, t)$ and $b \equiv b(x, t)$ are complex dynamical variables whose behavior is the subject of interest. Coefficients at linear terms undergo periodic variation with period T and amplitude A . The parameter modulation takes place in opposite phase for a and b . When the first subsystem is excited, the second one is relaxed and vice versa. The forcing is supposed to be slow, i.e., a half of period $T/2$ is much longer than a transient time of the excitation. The second terms in the right-hand parts of the equations provide saturation of instabilities in the excited subsystems. Additionally, there are terms responsible for coupling between the components a and b ; the intensity of the coupling is controlled by ϵ . The coupling is asymmetric: this is quadratic from a to b and linear in the reverse direction. Finally, the last terms in the right-hand parts introduce the diffusion, determining spatial distribution of the local oscillations. The diffusion coefficients of the subsystems are taken to be identical and equal to 1. We study the system in a limited spatial domain $0 \leq x \leq L$. The boundary conditions are

$$(\partial_x a)|_{x=0,L} = (\partial_x b)|_{x=0,L} = 0. \quad (3)$$

Let us briefly discuss a local dynamics of the system. Consider Eqs. (1). (A more detailed study can be found in Ref. [6].) Due to the presence of periodic forcing in (1), it is natural to introduce a stroboscopic map: we split the continuous time into steps of length T , and consider a sequence of states of the system at the beginnings of these steps. Define phases within the interval $[0, 2\pi)$: $\phi = \arg a$, $\psi = \arg b$. Suppose at some instant the first oscillator is excited and its amplitude $|a|$ is high. Then, the second one is suppressed, and its amplitude $|b|$ is small. The coefficients in (1) are real, except the coupling term. It means that the phases can vary only as a result of interaction between the subsystems. But, when a is excited, $|b|$ is small, and its action on a is negligible. Thus, the phase of a remains approximately constant during the excitation stage. On the contrary, the influence of the excited a on the suppressed b is strong. The coupling term is proportional to a^2 . It means that after a half period $T/2$ the oscillator b , at the threshold of its own excitation, inherits a doubled phase of a (also the phase gets a shift $-\pi/2$ because of the imaginary coefficient at the coupling term). Now the roles of the subsystems are exchanged. The phase of b remains constant when this subsystem is excited and at the end, after the other $T/2$, the phase is returned back to a through a linear coupling term (also with the shift $-\pi/2$). As a result, the first oscillator a doubles its phase during the period T . This discussion allows to write down a map for a series of phases $\phi_n = \arg a(nT)$ that are measured over the time step T :

$$\phi_{n+1} = 2\phi_n - \pi \pmod{2\pi}. \quad (4)$$

Up to a constant term (that can be eliminated by a shift of the origin of the phase) this map coincides with the well known Bernoulli map [13, 14]. It demonstrates chaotic dynamics, and the chaos is homogeneous: a rate of exponential divergence of two close trajectories is identical at each point of the phase space, being equal to $\ln 2$. Hence, getting back to the continuous system (1), we estimate its largest Lyapunov exponent as

$$\lambda_0 = \ln 2/T. \quad (5)$$

The described mechanism of phase doubling presumes a hyperbolic nature of the dynamics. The numerical verification of the cone criterion, that has been performed in [6], confirms this.

Before starting an analysis of the system (2), let us discuss a numerical method applied to find its solutions. Formally, our equations can be classified as parabolic PDE. Typical recommendation of handbooks for such equations is the Crank-Nicolson method which is absolutely stable and provides the second order of local approximation both in space and in time. This method is semi-implicit, i.e., a solution at new level t_{k+1} is implicitly expressed as a set of algebraic equations via previous solution at t_k . If PDE is linear, these equations are linear too. But application of this approach to nonlinear

PDEs, like ours, gives rise a set of nonlinear algebraic equations that require much more computational efforts. Usually, one simplifies the problem by neglecting terms, being nonlinear with respect to unknown variables. The resulting numerical scheme is semi-implicit for linear part of initial PDE and explicit for nonlinear part. Unfortunately, this simplified “quasi Crank-Nicolson” method is not absolutely stable. Sometimes everything goes fine, but sometimes, usually when the system is far beyond the instability threshold, the solution diverges. In this paper we do not neglect the nonlinearity and develop a true semi-implicit scheme. At each time step we solve a set of nonlinear equations via the Newton-Raphson iterations. The seed for the iterations is found from the mentioned simplified method. The iterations converge very fast. Normally, it takes 2 or 3 repetitions to solve the nonlinear equations with the accuracy 10^{-5} or even better. The idea of the described method can be found in books on numerical analysis, e.g., [15, 16]. Though the method is a bit complicated, this is compensated by its high accuracy and stability.

Below different characteristic values are calculated as functions of the length of the system L . Varying L , we need to choose some strategy of simultaneous variation of parameters of a numerical mesh. One way is to keep constant number of points of the mesh N and compute space step as $\Delta x = L/(N - 1)$. The other way is to fix the step Δx and find N for each L as $N = 1 + \lceil L/\Delta x \rceil$, where $\lceil \cdot \rceil$ means ceiling (to get a consistent numerical scheme one also needs to adjust actual value of Δx for the equality $\Delta x(N - 1) = L$ to fulfill). In our simulations we always keep constant N . This strategy is preferable because the number of degrees of freedom of the numerical model remains constant; obviously, it is equal to $4N$. So, we can be sure that phenomena, observed when L is varied, emerge due to a transformation of an inner structure of attractor, and they can not be attributed to just an extensive increase of degrees of freedom. The time step Δt can be either constant or attached to Δx . When the length is small, these two ways result in different behavior of analyzed dependencies. But in all cases these differences do not affect essential properties. So, in the course of simulations we prefer to keep constant time step, normally $\Delta t = 0.1$, but an alternative way will also be checked, and the differences will be discussed.

II. LINEAR STABILITY ANALYSIS

Standard linear stability analysis of autonomous spatially extended active system requires a consideration of small perturbations to a homogeneous steady state. Existence of perturbation modes with positive growth rates indicates that the homogeneous state is unstable. Our system does not have a steady state, and its dynamics is chaotic in time. Oscillations can be either homogeneous or irregular in space. Our aim is to find the conditions for a transition from one regime to another, utilizing ideas

of the standard analysis.

Suppose that the system is infinite in space and its initial state is uniform. Prepared in this way, the system obviously demonstrates homogeneous oscillations; at any spatial point the dynamics can be described by the ODE system (1). Let us consider an inhomogeneous perturbation to these oscillations. We need to seek a solution composed as a sum of a homogeneous part, say, $a_0(t)$ and $b_0(t)$, and a sinusoidal mode of perturbation with real wave number k and real growth rate $\sigma(k)$. The system is chaotic; thus, instead of usual assumption of time periodicity of small perturbation, we introduce small amplitudes $\tilde{a}(t)$ and $\tilde{b}(t)$ and require them neither grow, nor decay in average. It means that there exist two constants, $0 < K < M < \infty$, such that $K < |\tilde{a}(t)| < M$ and $K < |\tilde{b}(t)| < M$ for $t > 0$. So, we set:

$$\begin{aligned} a(x, t) &= a_0(t) + \tilde{a}(t)e^{\sigma(k)t - ikx}, \\ b(x, t) &= b_0(t) + \tilde{b}(t)e^{\sigma(k)t - ikx}. \end{aligned} \quad (6)$$

After substitution (6) to (2), we exclude nonlinear terms in \tilde{a} and \tilde{b} , supposed to be small, and obtain a set of linear ODE for complex amplitudes of perturbation:

$$\begin{aligned} \dot{\tilde{a}} &= (A \cos(2\pi t/T) - \lambda_0)\tilde{a} - 2|a_0|^2\tilde{a} - a_0^2\tilde{a}^* - i\epsilon\tilde{b}, \\ \dot{\tilde{b}} &= (-A \cos(2\pi t/T) - \lambda_0)\tilde{b} - 2|b_0|^2\tilde{b} - b_0^2\tilde{b}^* - 2i\epsilon a_0\tilde{a}, \end{aligned} \quad (7)$$

where $\lambda_0 = k^2 + \sigma(k)$ and asterisk denote the complex conjugation. A value of λ_0 controls growth or decay of a solution. Because $\tilde{a}(t)$ and $\tilde{b}(t)$ should be bounded at any k , λ_0 does not depend on k . One can easily check that (7) also describes small perturbation to an orbit of (1). It means that the conditions on $\tilde{a}(t)$ and $\tilde{b}(t)$ are fulfilled when λ_0 is equal to the largest Lyapunov exponent of (1). Thus, we can write

$$\sigma(k) = \lambda_0 - k^2. \quad (8)$$

Relation (8) can be verified by direct numerical computations of $\sigma(k)$. For this purpose we substitute $\lambda_0 = \sigma(k) + k^2$ to (7) and set there $\sigma(k) = 0$. It means that now the amplitudes \tilde{a} and \tilde{b} are allowed to grow or decay, and the rate is equal to $\sigma(k)$. Given k , we find $\sigma(k)$ employing the algorithm of computing of the largest Lyapunov exponent [17]. System (7) is initialized with a unit vector, and then solved together with (1) on one period T . After that, a norm of vector-solution of (7) is found, and the vector is normalized. When this procedure is repeated for a sufficiently long time interval, the average logarithms of the norms determine the sought $\sigma(k)$. The results are shown in Fig. 1. Solid lines represent theoretical $\sigma(k)$ (8). The upper one corresponds to a hyperbolic chaos in (1) and λ_0 is found according to (5). The lower curve also corresponds to chaotic oscillations of (1), that are, however, non-hyperbolic. In this case we substitute a computed value of $\sigma(0)$ to (8) instead of λ_0 . Numerical data fit well the theoretical curves. As follows from (8)

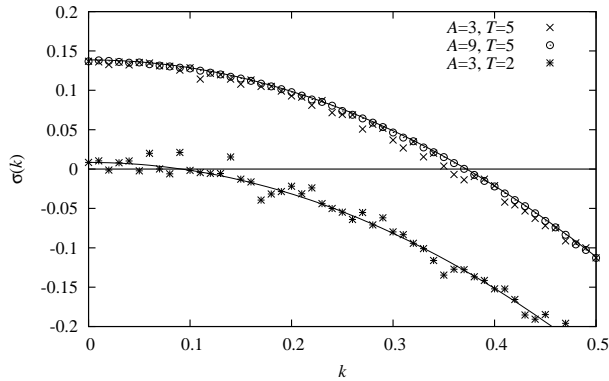


Figure 1: Growth rate $\sigma(k)$ of nonuniform perturbation to a homogeneous solution of the system (2). The solid curves are the graphs of (8): the upper one is $(\ln 2)/5 - k^2$, the lower one is $\sigma(0) - k^2$, where $\sigma(0) = 0.00842$. Crosses, circles and stars represent numerical data, computed at parameters that are shown in the legend.

and (5), $\sigma(k)$ does not depend on the A in the regime of hyperbolic chaos. Numerical verification confirms this.

Linear modes described by (7) are influenced parametrically by a chaotic force. All modes with positive $\sigma(k)$ can grow simultaneously that results in a spatiotemporal chaos. The spectrum of linearly unstable modes with $\sigma(k) > 0$ can be found from (8). These modes lay within the interval of wave numbers $0 \leq k < k_{\text{lin}}$, where

$$k_{\text{lin}} = \sqrt{\lambda_0}. \quad (9)$$

If the system (2) is spatially bounded of length L , the spectrum of modes allowed by the boundary conditions (3) is

$$k_n = n\pi/L, \quad n = 1, 2, 3, \dots \quad (10)$$

When L is small, so that $k_1 > k_{\text{lin}}$, there are no unstable eigenmodes. The system demonstrates homogeneous oscillations. The spatial structure emerges above the critical point which can be found from the condition $k_1 = k_{\text{lin}}$: $L_c = \pi/\sqrt{\lambda_0}$. Below we put attention to the case when the local dynamics is hyperbolic. The Lyapunov exponent λ_0 in this case is given by (5) and the critical length reads:

$$L_c = \pi\sqrt{T/\ln 2}. \quad (11)$$

III. SPATIOTEMPORAL DYNAMICS

Let us consider some illustrations of spatiotemporal dynamics of the system (2). Figure 2 represents homogeneous oscillations. In this and subsequent figures a space coordinate is horizontal, time is directed vertically and grey levels indicate values of $\text{Re } a$ as shown by a gradient bar at the right edge of diagram. Time is discrete: layers $\text{Re } a(x)$ are plotted at successive steps $t_n = nT$. Critical

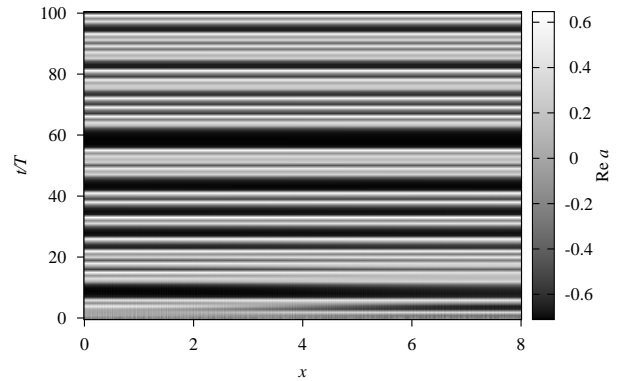


Figure 2: Spatiotemporal dynamics of (2) at $L = 8$. Grey levels indicate values of $\text{Re } a$. $A = 3$, $T = 5$, $\epsilon = 0.05$.

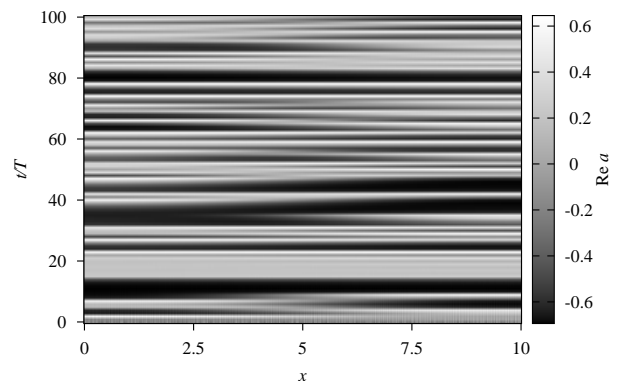


Figure 3: Same as Fig. 3, but at $L = 10$.

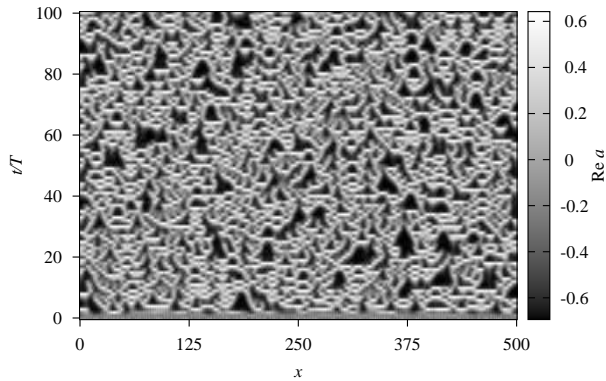
length, according to (11), is $L_c \approx 8.44$. The length of the system in Fig. 2 is less than the critical value, $L = 8$. Hence, after a short transient time, it settles in a regime of homogeneous oscillations.

In Fig. 3 the length $L = 10$ is larger than L_c . The first eigenmode $\cos(k_1 x)$ falls into the instability domain and grows, destroying the homogeneity. The first mode contains one half of the period of cosine, so if a maximum is at the left edge of the system, a minimum appears at the right edge and vice versa. Careful inspection of Fig. 3 confirms this conclusion. If a horizontal stripe, representing $\text{Re } a(x)$ at a certain time step, is white at the left edge, it becomes dark at the right edge.

The result of further increase of the length up to $L = 500$ is shown in Fig. 4. As here a lot of eigenmodes satisfy the condition $k_n < k_{\text{lin}}$, they are excited and produce a rich and complicated structure. It is interesting to note that it reminds a structure generated by a cellular automata of Wolfram's class 3 [18].

IV. LYAPUNOV ANALYSIS

Lyapunov exponents are average rates of expansion or contraction in the tangent space on an attractor. They

Figure 4: $L = 500$.

characterize the sensitivity of motion to small perturbations; an attractor with a positive exponent is chaotic. Also, it is important to know a mutual orientation of expanding and contracting directions in the tangent space at each point of the attractor. This information can be provided by covariant Lyapunov vectors [12]. If there is a well defined split of the tangent space into stable and unstable subspaces, the dynamics is hyperbolic. On the contrary, the dynamics is non-hyperbolic when couples of collinear vectors from stable and unstable subspaces can be encountered with a nonzero probability.

In these section we compute covariant Lyapunov vectors and perform a verification of hyperbolicity of the attractor of (2). Also we analyze Lyapunov exponents for the system (2) as well as related to them Kaplan-Yorke dimension and Kolmogorov-Sinai entropy.

A. Verification of hyperbolicity at different lengths of the system

To verify the hyperbolicity one needs to analyze expanding and contracting directions in the tangent space on an attractor. These directions can be found in a form of covariant Lyapunov vectors [12]. The method of computation of these vectors is briefly described in the appendix.

When the covariant Lyapunov vectors are computed at some point of an attractor, one can look through each couple of expanding and contracting vectors and find those which have the smallest angle. Collecting these angles for sufficiently many points, one obtains a sufficient condition for non-hyperbolicity: the attractor is non-hyperbolic if zero angle can be encountered with nonzero probability. But the converse is not true. The covariant Lyapunov vectors themselves may not be collinear, but the loss of hyperbolicity still can take place due to a tangency of some arbitrary couple of vectors from stable and unstable subspaces, respectively. To take this situation into account, we suggest the following procedure.

Let us suppose that at some point of the attractor we have covariant Lyapunov vectors s_i , $i = 1, 2, \dots, n_s$, as-

sociated with the stable subspace of the tangent space, and u_i , $i = 1, 2, \dots, n_u$, associated with the unstable subspace. The total number of vectors $n_s + n_u$ is equal to the dimension of the tangent space. Two generic vectors g_s and g_u can be defined inside these subspaces as

$$g_s = G_s \alpha, \quad g_u = G_u \beta, \quad (12)$$

where $\alpha \in \mathbb{R}^{n_s}$, $\beta \in \mathbb{R}^{n_u}$, $G_s = \{s_1, s_2, \dots, s_{n_s}\} \in \mathbb{R}^{(n_s+n_u) \times n_s}$, and $G_u = \{u_1, u_2, \dots, u_{n_u}\} \in \mathbb{R}^{(n_s+n_u) \times n_u}$. If all s -vectors are linearly independent, α contains n_s unknown coordinates of g_s with respect to the basis G_s . But if some of s -vectors can be expressed as linear combinations of other vectors, we assume that corresponding components of α are zeros. Similarly, components of β , corresponding to linearly dependent u -vectors, are also zeros. Thus, α contains $n_p \leq n_s$ nonzero unknown components, and β consists of $n_q \leq n_u$ nonzero components.

In terms of these definitions, to verify the hyperbolicity we need to find g_s and g_u having the minimal angle. The hyperbolicity is lost if the angle vanishes. This can be formulated as an optimization problem:

$$g_s^T g_s = 1, \quad g_u^T g_u = 1, \quad g_s^T g_u = f, \quad (13)$$

where f is a function of g_s and g_u that should be maximized. Substituting (12) to (13), we obtain:

$$\alpha^T G_s^T G_s \alpha = 1, \quad \beta^T G_u^T G_u \beta = 1, \quad \alpha^T G_s^T G_u \beta = f. \quad (14)$$

The matrix $G_s^T G_s$ is real, symmetric and non-negative definite. Thus, there exists the decomposition $G_s^T G_s = D_s \Lambda_s^2 D_s^T$ [19], where $D_s \in \mathbb{R}^{n_s \times n_s}$ is real orthogonal matrix, and $\Lambda_s^2 \in \mathbb{R}^{n_s \times n_s}$ is real diagonal matrix with elements $\ell_1^2 \geq \ell_2^2 \geq \dots \geq \ell_{n_p}^2 > 0$, $\ell_{j(>n_p)} = 0$. If $n_p < n_s$, the last $n_s - n_p$ columns of D_s are multiplied by zeros and do not give any contribution to $G_s^T G_s$. The insignificant components can be omitted to obtain an equivalent relation $G_s^T G_s = \tilde{D}_s \tilde{\Lambda}_s^2 \tilde{D}_s^T$, where $\tilde{D}_s \in \mathbb{R}^{n_p \times n_p}$ is the D_s without last $n_s - n_p$ columns, and $\tilde{\Lambda}_s^2 \in \mathbb{R}^{n_p \times n_p}$ is the upper left block of Λ_s^2 without zeros on the diagonal. Similarly, $G_u^T G_u = \tilde{D}_u \tilde{\Lambda}_u^2 \tilde{D}_u^T$, where $\tilde{D}_u \in \mathbb{R}^{n_u \times n_u}$ is a matrix with n_q orthogonal columns, and $\tilde{\Lambda}_u^2 \in \mathbb{R}^{n_q \times n_q}$ is diagonal matrix with positive elements. Taking these decompositions into account, we can introduce new variables $\alpha_1 = \tilde{\Lambda}_s \tilde{D}_s^T \alpha$, and $\beta_1 = \tilde{\Lambda}_u \tilde{D}_u^T \beta$, where $\alpha_1 \in \mathbb{R}^{n_p}$ and $\beta_1 \in \mathbb{R}^{n_q}$. This variables change is reversible because α and β also contain n_p and n_q nonzero components, respectively. In these variables (14) has a form

$$\alpha_1^T \alpha_1 = 1, \quad \beta_1^T \beta_1 = 1, \quad \alpha_1^T M \beta_1 = f, \quad (15)$$

where $M \in \mathbb{R}^{n_p \times n_q}$,

$$M = \tilde{\Lambda}_s^{-1} \tilde{D}_s^T G_s^T G_u \tilde{D}_u \tilde{\Lambda}_u^{-1}. \quad (16)$$

Matrix M allows the singular value decomposition $M = U W V^T$ [19], where $U \in \mathbb{R}^{n_p \times n_p}$ and $V \in \mathbb{R}^{n_q \times n_q}$ are real orthogonal matrices, and $W \in \mathbb{R}^{n_p \times n_q}$ is diagonal matrix whose elements $w_1 \geq w_2 \geq \dots \geq w_r > 0$,

$w_{j(>r)} = 0$, $r \leq \min\{n_p, n_u\}$, are the singular values of M . Because U and V are orthogonal, the variables change $\alpha_2 = U^T \alpha_1$, $\beta_2 = V^T \beta_1$ in (15) can be performed to obtain the following equations:

$$\alpha_2^T \alpha_2 = 1, \quad \beta_2^T \beta_2 = 1, \quad \alpha_2^T W \beta_2 = f. \quad (17)$$

Only r diagonal elements of the W are not equal to zero. It means that only r components of α_2 and β_2 can influence f , while all the rest components can be assumed to be zero and omitted:

$$\alpha_3^T \alpha_3 = 1, \quad \beta_3^T \beta_3 = 1, \quad \alpha_3^T \tilde{W} \beta_3 = f, \quad (18)$$

where $\alpha_3 \in \mathbb{R}^r$, $\beta_3 \in \mathbb{R}^r$, $\tilde{W} \in \mathbb{R}^{r \times r}$. Finally, the last change of variables $\alpha_4 = \tilde{W} \alpha_3$ results in the equations

$$\alpha_4^T \tilde{W}^{-2} \alpha_4 = 1, \quad \beta_3^T \beta_3 = 1, \quad \alpha_4^T \beta_3 = f. \quad (19)$$

Our problem in terms of Eqs. (19) sounds as follows: we need to find a vector α_4 on the surface of an ellipsoid and a vector β_3 on the surface of a sphere such that their inner product is the largest. It is obvious, that α_4 should coincide with the largest semi-axis of the ellipsoid and β_3 should be collinear to α_4 . In this case the maximum is $f = w_1$ and the sought minimal angle between the vectors g_s and g_u is

$$\theta = \arccos w_1. \quad (20)$$

The other singular values of M bring additional information about the structure of the tangent space. In particular, if a system has many degrees of freedom, several couples of vectors from the stable and unstable subspaces can have zero angle. The number of such linearly independent couples defines a dimension of the tangency. Analyzing Eqs. (19), one can see that the dimension of the tangency is equal to the number of largest singular values that are equal to 1.

So, being at some point of attractor, we need to construct the matrix M (16). Arc cosine of its largest singular value is the angle θ , characterizing a mutual orientation of the stable and unstable subspaces at this point. To verify the hyperbolicity, we need to find a distribution of these angles on the attractor. The necessary and sufficient condition for the loss of hyperbolicity is vanishing of θ with a nonzero probability.

The described method can be easily implemented as a computer program. In fact, when the covariant Lyapunov vector are obtained, one needs to compute eigenvalues and eigenvectors of the real symmetric matrices $G_s^T G_s$ and $G_u^T G_u$ and then find the singular value decomposition of the real matrix M . Both of the procedures have efficient numerical algorithms, which can be found in textbooks, e.g., in Refs [19, 20].

Figure 5 represents distributions of angles θ for the system (2) at different lengths L . The distributions are computed with resolution 300 points; 20 trajectories of length 500 are processed to collect the angles for each distribution. Equations are solved at $N = 101$ points of

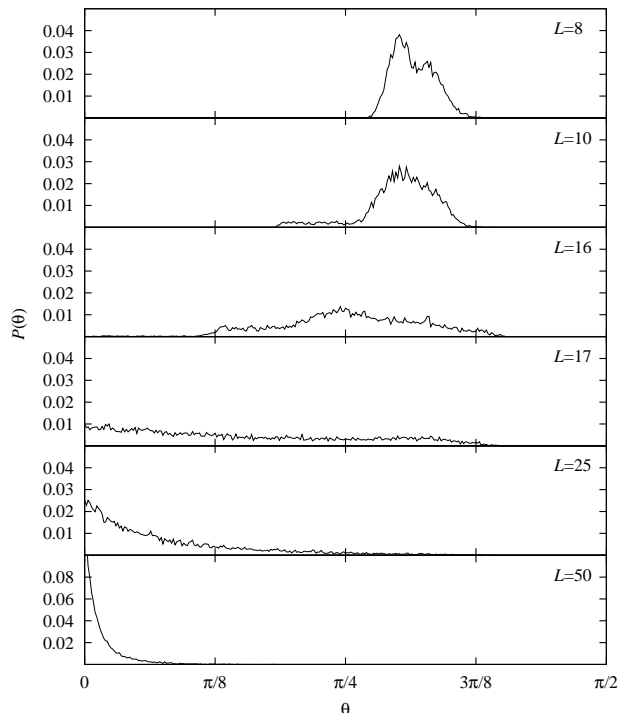


Figure 5: Distributions of minimal angles θ (20) between stable and unstable subspaces in the tangent space of the attractor of (2). $A = 3$, $T = 5$, $\epsilon = 0.05$. Observe the violation of hyperbolicity at $L > 16$.

spatial discretization, i.e., there are 404 covariant Lyapunov vectors of length 404. Time step is $\Delta t = 0.1$. The distributions are normalized, $\int_0^{\pi/2} P(\theta) d\theta = 1$.

The upper curve $L = 8$ in Fig. 5 illustrates a spatially homogeneous case. The distribution is very well localized within the interval of angles $\pi/4 < \theta < 3\pi/8$. It means that the hyperbolic dynamics is observed that corresponds to the hyperbolic dynamics of the ODE system (1). The second curve $L = 10$ represents a case of a weak inhomogeneity, when the system is not far above the critical point L_c . Though this is qualitatively different type of behavior, in the phase space the system remains close to the spatially homogeneous attractor. Form of the distribution is similar to the previous case, except a small plateau attached at the left foot of the main hill. This plateau is a manifestation of small deviations from the homogeneous attractor. On the third curve $L = 16$ we still can discern the main hill and the plateau. The curve is much lower and wider than two previous, but zero angles are not encountered, i.e., the hyperbolicity survives. The distribution becomes dramatically different at $L = 17$ that presumes some bifurcation on the interval $16 < L < 17$. The part of the curve, formerly termed as the plateau, now looks like a slope, and it touches the origin. It means that the dynamics is non-hyperbolic any more. The rests of the main hill are still distinguishable, but at higher L they disappear at all.

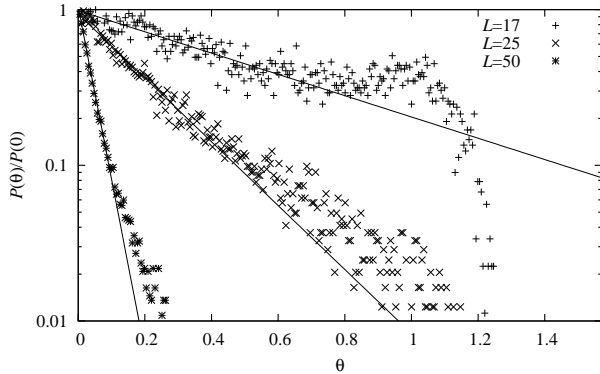


Figure 6: Distributions of angles θ in logarithmic scale. Solid lines are obtained via least squares fit. The data sets are the same as in Fig. 5

The distributions at $L = 25$ and $L = 50$ have maxima at the origin, and they demonstrate monotonic decay. Notice also the high smoothness of the curve at $L = 50$. Figure 6 reproduces the distributions, computed above the point of hyperbolicity loss, in logarithmic scale. Near the origin the numerical data are approximated well by straight lines that implies exponential dependence. In the other words, behind the point of hyperbolicity loss the angles θ obey an exponential distribution, and, as follows from Figs. 5 and 6, the argument of the exponential function grows in absolute value with L . Because of huge time of computations required, the law of this growth is unclear yet. In particular, it is interesting to know, if the exponent diverges as $L \rightarrow \infty$ or tends to a finite limit.

Below we demonstrate that the loss of hyperbolicity takes place when the third Lyapunov exponent passes zero.

B. Lyapunov exponents against the length of the system

Figure 7 represents Lyapunov exponents as functions of L . The plots are obtained at $N = 301$ and $\Delta t = 0.1$. The choice for Δt to be constant determines the vanishing of the negative exponents as $L \rightarrow 0$. If the equality $\Delta t = \Delta x$ is held instead, all negative exponents have identical nonzero values at the origin.

The largest exponent λ_0 remains almost constant as L varies, see the lower panel in Fig. 7. The approximating line, obtained via the least squares fit at $L_c < L < 55$, does not have a noticeable slope and is plotted at constant value 0.1386. This is equal with remarkable accuracy to the theoretically predicted largest Lyapunov exponent (5) of the corresponding ODE system (1).

When L is small, the system has one positive exponent that corresponds to spatially homogeneous chaotic oscillations. As L grows, the second exponent λ_1 becomes positive at $L = L_c$. This indicates the transition to a

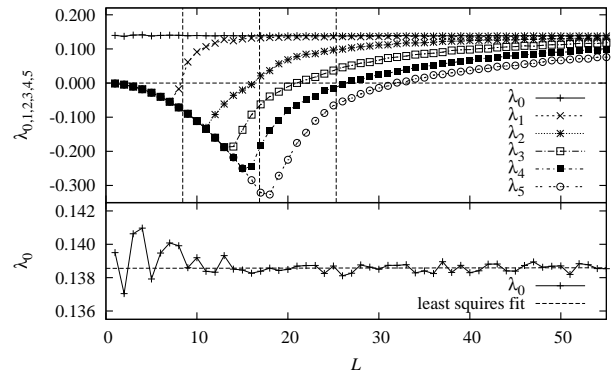


Figure 7: Six largest Lyapunov exponents of the system (2) against L . $A = 3$, $T = 5$, $\epsilon = 0.05$. Vertical dashed lines mark $L_c \approx 8.44$, $2L_c$ and $3L_c$. Lower panel represents λ_0 in a large scale. The dashed approximating line $6 \times 10^{-7}L + 0.1386$ is obtained via least squares fit at $L_c < L \leq 55$.

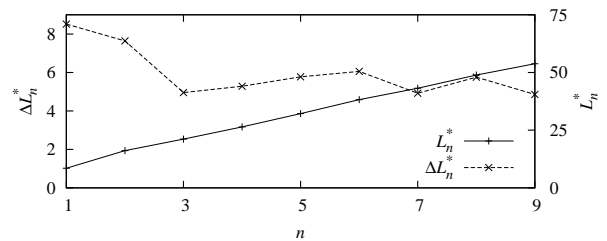


Figure 8: Values of length L_n^* where Lyapunov exponents pass through zero, and intervals between these points $\Delta L_n^* = L_n^* - L_{n-1}^*$ ($L_0^* \equiv 0$ by default). Parameters are as in Fig. 7.

spatially inhomogeneous solution. Further increase of L results in a cascade of passing through zero of the exponents. Fig. 8 shows zeros of the exponents L_n^* and the intervals between successive points $\Delta L_n^* = L_n^* - L_{n-1}^*$ ($L_0^* \equiv 0$ by default) against the number of exponent n . One can see that L_n^* linearly depends on n . It means that the number of positive exponents also linearly, on average, depends on L .

Notice that $L_2^* = 16.2$ falls in the interval $16 < L < 17$ where the loss of hyperbolicity takes place. We can guess that L_2^* is the point of the loss, i.e., the violation of hyperbolicity takes place when the third Lyapunov exponent passes through zero. One can see that ΔL_1^* and ΔL_2^* in Fig. 8 distinctly differ from all others ΔL_n^* . This can be explained by a transformation which undergoes the attractor at L_2^* .

C. Kaplan-Yorke dimension and Kolmogorov-Sinai entropy

Figure 9 represents Kaplan-Yorke or Lyapunov dimension D_{KY} [13, 14], and the sum of positive exponents h'_μ , which is an upper estimate for the Kolmogorov-Sinai or metric entropy [13, 14]. The divergence of the D_{KY} as

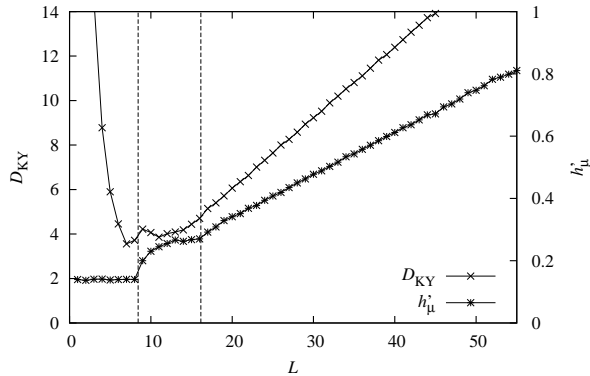


Figure 9: Kaplan-Yorke dimension D_{KY} and upper estimate h'_μ for the Kolmogorov-Sinai entropy against L . Parameters are as in Fig. 7. Vertical dashed lines mark $L_c \approx 8.44$ and $L_2^* \approx 16.2$.

$L \rightarrow 0$ is a consequence of the vanish of negative Lyapunov exponents at the origin, see Fig. 7. As mentioned above, this takes place because Δt is constant while Δx is varied with L . If the relation $\Delta t/\Delta x$ is held, the dimension has a finite nonzero value at the origin.

Vertical dashed lines in Fig. 9 mark L_c and L_2^* . Observe that below L_2^* both D_{KY} and h'_μ are nonlinear functions of L , while above this point they grow linearly. This agrees with the suggestion that the attractor undergoes a transformation at $L = L_2^*$.

Linear growth of D_{KY} and h'_μ against L in Fig. 9, and also the linear growth of the number of positive exponents, which follows from the linear growth of L_n^* in Fig. 8, can be explained by exponential decay of spatial correlation. Two points distant further than the correlation length move independently, so that the system can be roughly approximated as a direct product of independent subsystems [21]. Thus, the additivity is observed: the increment of L merely results in the proportional increasing of the characteristic values. A good estimate for the correlation length is the distance between zero crossing points of the Lyapunov exponents ΔL_n^* , which is almost constant as seen from Fig. 8.

Such behavior is typical for fully developed chaos in extended systems. In particular, the linear growth of $D_{KY}(L)$ and $h'_\mu(L)$ was reported for coupled map lattices [21], for Kuramoto-Sivashinsky (KS) equation [22] and for complex Ginzburg-Landau (CGL) equation [23]. Also, the linear growth of D_{KY} was demonstrated for a chaotic attractor of coupled Ginzburg-Landau equations [24].

Let us consider h'_μ in more details, see Fig. 10. It is known that for a hyperbolic attractor h'_μ is equal to Kolmogorov-Sinai entropy h_μ . For a generic chaotic attractor, however, h'_μ may not be equal to h_μ , but the inequality $h_\mu \leq h'_\mu$ is always valid [14]. Because our system is hyperbolic at $L < L_2^*$, we can use h'_μ to construct a function which approximates h_μ at least on this interval. In Fig. 10 the numerical data for h'_μ are plotted by pluses.

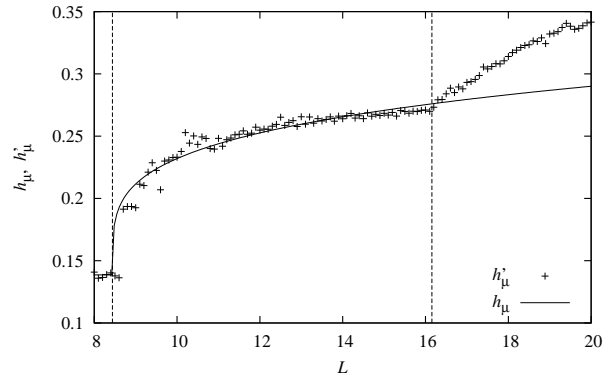


Figure 10: Approximation of Kolmogorov-Sinai entropy h_μ via least squares fit of h'_μ at $L < L_2^*$. Vertical dashed lines mark $L_c \approx 8.44$ and $L_2^* \approx 16.2$. Parameters are as in Fig. 7.

Below the point $L = L_c$ $h'_\mu = \lambda_0$, while above this point h'_μ demonstrates a power law behavior. Thus, employing the least squares fit, we obtain a function, approximating h_μ as

$$h_\mu(L) = \begin{cases} \lambda_0 & L \leq L_c, \\ 0.084(L - L_c)^{0.24} + \lambda_0 & L > L_c. \end{cases} \quad (21)$$

In Fig. 10 $h_\mu(L)$ is represented by a solid line. At $L = L_2^*$ a bifurcation occurs that, as we argue, is associated with the loss of hyperbolicity. There are two possibilities above this point. The first one is that h_μ is still described by (21), but, because the attractor is non-hyperbolic, h'_μ serves as an upper estimate, $h_\mu < h'_\mu$. The other possibility is that the equality $h_\mu = h'_\mu$ remains valid, while the approximation (21) becomes inappropriate. Anyway, both of these variants fit well with our conclusion that the system loses the hyperbolicity at $L = L_2^*$.

D. Spectra of Lyapunov exponents

Figure 11(a) demonstrates spectra of Lyapunov exponents at different L . The first curve $L = 8$ corresponds to a spatially homogeneous case when oscillations in all spatial points are synchronized and can be described by (1). The system (1) has four degrees of freedom, and we see that there are four different values of λ in the spectrum. All other exponents are equal to λ_3 . When L passes $L_c \approx 8.44$ the second positive exponent appears. This case is illustrated by the curve $L = 10$. At $L = 18$ we observe 3 positive exponents. Further growth of L brings more exponents to positive half-plane. At $L = 50$ there are 9 positive exponents.

Notice that spectra in Fig. 11(a) are clearly separated onto two parts. This is seen for $L = 8$ and $L = 10$. The first part contains all positive exponents and some of negative. And the second one contains a tail of identical values. As discussed in [25], the first part represents so called “physical” modes that carry all significant observable properties of the dynamics. The second part, on

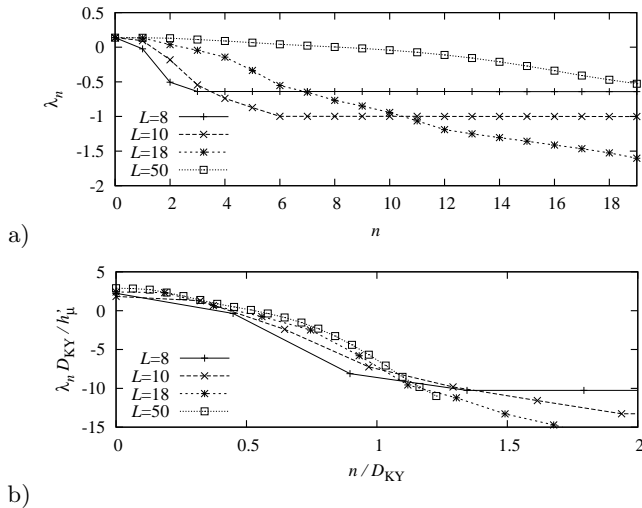


Figure 11: a) Spectra of Lyapunov exponents and b) the rescaled spectra at different lengths of the system. $A = 3$, $T = 5$, $\epsilon = 0.05$, $L_c \approx 8.44$. All the spectra have identical values $\lambda_0 = \log(2)/T$ at the origin.

the contrary, is associated with highly damped degrees of freedom that are not necessary to describe the dynamics.

Let us now discuss a scaled form of the spectrum $\lambda(n/D_{KY})D_{KY}/h'_\mu$. For a fully developed spatiotemporal chaos the scaled Lyapunov spectrum tends to a limiting curve as $L \rightarrow \infty$. In particular, this was reported for coupled map lattice [21], for Kuramoto-Sivashinsky (KS) equation [22] and for complex Ginzburg-Landau (CGL) equation [23]. Figure 11(b) represents the verification of this property for the system (2). One can see high correspondence of curves, obtained at different L . Because in our case the largest Lyapunov exponent remains constant, simple rescaled form $\lambda(n/D_{KY})$ also converges to a limiting curve.

V. SUMMARY AND CONCLUSION

We considered an extended system whose local dynamics is hyperbolic and spatial coupling is introduced via diffusion. A numerical verification of hyperbolicity of the attractor of this system was performed. The test was based on the computation of distributions of minimal angles between vectors belonging to stable and unstable subspaces of the tangent space of the attractor. The analysis showed that the hyperbolicity is inherent only to a low dimensional chaos observed at sufficiently small lengths of the system.

The dynamics is hyperbolic when oscillations are homogeneous in space. This regime is characterized by a single positive Lyapunov exponent. The hyperbolicity survives when the length gets larger, so that the first spatial mode, determined by boundary conditions, becomes linearly unstable, and the oscillations becomes inhomogeneous. This transition is accompanied by the emergence

of the second positive Lyapunov exponent. But further growth of the length results in the violation of hyperbolicity. This takes place when the third Lyapunov exponent passes through zero.

Beyond the point of the hyperbolicity loss, the system demonstrates an extensive spatiotemporal chaos that is characterized by a fast decay of a spatial correlation. We verified several standard criteria and observed behavior that is typical for many others extended chaotic systems. Namely, the number of positive Lyapunov exponents, the sum of positive exponents (this value is an upper estimate for Kolmogorov-Sinai entropy) and the Kaplan-Yorke dimension grow linearly against the length of the system. Spectrum of the Lyapunov exponents, being properly rescaled, tends to a limiting curve as the length grows.

Above the point of violation of hyperbolicity the distributions of minimal angles between stable and unstable tangent subspaces are exponential and have the maxima at the origin. The exponent of distribution grows with the length of the system. It is not clear yet does this exponent diverge or it tends to a finite limit. The divergence means that in the infinite system tangencies between stable and unstable subspaces take place almost at each point of the attractor. On the one hand, it seems to be a kind of total non-hyperbolicity. But in fact, because the system has infinite number of degrees of freedom, it is important to know the dimension of the tangencies. If the dimension remains finite when the number of degrees of freedom tends to infinity, the influence of the tangencies on the dynamics becomes insignificant, and the system is effectively hyperbolic. But if the dimension diverges, we obtain essentially different situation. This requires a further detailed investigation which will be performed in our subsequent study.

Acknowledgments

The authors acknowledge support from RFBR-DFG grant No 08-02-91963.

Appendix: COMPUTING OF LYAPUNOV EXPONENTS AND COVARIANT LYAPUNOV VECTORS

To compute Lyapunov exponents, we apply an algorithm based on the QR -decomposition. See Refs. [26, 27, 28] for the details of the algorithm, and Ref. [19] for an idea of the QR -decomposition. The method of computation of covariant Lyapunov vectors is recently reported in Ref. [12]. This also employs the QR -decomposition.

First of all, equations for small perturbations $\tilde{a}(x, t)$ and $\tilde{b}(x, t)$ to a trajectory $a(x, t)$ and $b(x, t)$ of (2) are

required:

$$\begin{aligned}\partial_t \tilde{a} &= A \cos(2\pi t/T) \tilde{a} - 2|a|^2 \tilde{a} - a^2 \tilde{a}^* - i\tilde{e}\tilde{b} + \partial_x^2 \tilde{a}, \\ \partial_t \tilde{b} &= -A \cos(2\pi t/T) \tilde{b} - 2|b|^2 \tilde{b} - b^2 \tilde{b}^* - 2i\tilde{e}a\tilde{a} + \partial_x^2 \tilde{b},\end{aligned}\tag{A.1}$$

where asterisk denotes the complex conjugation. To compute M_λ Lyapunov exponents, we need M_λ exemplars of the linear equation sets (A.1), which are initialized by an orthogonal set of random unit vectors of the length $4N$, where N is a number of points of numerical mesh. Basic system (2) is also initialized and advanced along a trajectory for sufficiently long time to arrive at the attractor. Then the basic system is solved simultaneously with M_λ linear equation sets on one period of time T . M_λ resulting vectors are considered as columns of a matrix that is decomposed into an orthogonal matrix Q and an upper-triangular matrix R . (An algorithm based on the Householder rotation is used [19].) Logarithms of M_λ diagonal elements of the R are collected, while M_λ columns of the Q are used to re-initialize linear systems. Then this procedure is repeated. Averaged logarithms of diagonal elements of R converge to Lyapunov exponents.

To compute covariant Lyapunov vectors, we must do the similar things. After initialization, we make sufficiently many steps n_0 accompanied by the QR -procedure, but without storing diagonal elements of R , to obtain a good matrix Q_{n_0} . ‘‘A good’’ means that each linear subspace $S_{n_0}^j$, $j = 1, 2, \dots, 4N$, spanned by first j vector-columns of Q_{n_0} , contains j -th unstable (or stable) direction of the tangent space at n_0 . Starting from n_0 , we make some more steps, storing each Q_n and R_n , and arrive at n_1 . Here we have a matrix Q_{n_1} with columns that determine subspaces $S_{n_1}^j$. Our aim now is to define arbitrary unit vectors belonging to these subspaces, $u_{n_1}^j \in S_{n_1}^j$, $j = 1, 2 \dots 4N$. In fact, we just need to gen-

erate a random upper-triangular matrix C_{n_1} , whose size coincides with R , and columns are normalized by 1. j -th column of C_{n_1} contains coordinates of $u_{n_1}^j$ with respect to the basis Q_{n_1} . In the other words

$$U_n = Q_n C_n,\tag{A.2}$$

where $U_n = \{u_n^1, u_n^2, \dots, u_n^{4N}\}$. Starting from C_{n_1} , we perform backward iterations $C_{n-1} = R_n^{-1} C_n$, performing re-normalization of columns of C_n after each step. Collecting and averaging the negative logarithms of the norms, we obtain Lyapunov exponents. It easy to verify that these iterations are equivalent to solving of the linear equation sets in backward time with U_{n_1} as an initial state. It means that under the iterations the vectors u_n^j , represented by columns of the C_n , are aligned with the most expanding directions of subspaces S_n^j . These directions are associated with corresponding Lyapunov exponents. Because we go back in time, the highest Lyapunov exponents do not dominate this alignment. If the number of steps from n_1 to n_0 is sufficiently large, getting back at n_0 , we obtain the matrix C_{n_0} with coordinates of covariant Lyapunov vectors U_{n_0} , which point expanding and contracting directions of the tangent space at n_0 . Explicit form of U_{n_0} can be found from (A.2). Computed in parallel, the Lyapunov exponents allow to distinguish expanding and contracting directions. Now, because all Q_n and R_n are stored, we can compute and store the next couple corresponding to the step $n_1 + 1$ and, after the backward procedure, obtain a set of covariant Lyapunov vectors at the point $n_0 + 1$. In this way we can compute the vectors along the trajectory. Notice that this procedure allows to compute not only all $4N$ vectors, but any first $M_\lambda \leq 4N$ required vectors.

-
- [1] A. Katok and B. Hasselblatt, *Introduction to the modern theory of dynamical systems* (Cambridge University Press, 1995).
- [2] J. Guckenheimer and P. Holmes, *Nonlinear oscillations, dynamical systems, and bifurcations of vector fields* (Springer, 2002).
- [3] S. P. Kuznetsov, Phys. Rev. Lett. **95**, 144101 (2005).
- [4] S. P. Kuznetsov and E. P. Seleznev, JETP **102**, 355 (2006).
- [5] S. P. Kuznetsov and I. R. Sataev, Phys. Lett. A **365**, 97 (2007).
- [6] P. V. Kuptsov, S. P. Kuznetsov, and I. R. Sataev, *Hyperbolic attractor of Smale-Williams type in a system of two coupled non-autonomous amplitude equations*, arXiv:0804.3677 (2008).
- [7] O. B. Isaeva, A. Y. Jalnina, and S. P. Kuznetsov, Phys. Rev. E **74**, 046207 (2006).
- [8] S. P. Kuznetsov and A. Pikovsky, Physica D **232**, 87 (2007).
- [9] S. P. Kuznetsov and A. Pikovsky, Europhysics Letters **28**, 10013 (2008).
- [10] S. P. Kuznetsov and V. I. Ponomarenko, Tech. Phys. Lett. **34**, 771 (2008).
- [11] L. Young, Nonlinearity **21**, T245T252 (2008).
- [12] F. Ginelli, P. Poggi, A. Turchi, H. Chaté, R. Livi, and A. Politi, Phys. Rev. Lett. **99**, 130601 (2007).
- [13] H. G. Schuster, *Deterministic chaos: an introduction* (Physik Verlag, Weinheim, 1984).
- [14] E. Ott, *Chaos in dynamics systems* (Cambridge University Press, 1993).
- [15] N. N. Kalitkin, *Chislennyye metody (Numerical methods, in russian)* (Moscow, Nauka, 1978).
- [16] W. F. Ames, *Numerical methods for partial differential equations* (Academic Press, 1977).
- [17] T. S. Parker and L. O. Chua, *Practical numerical algorithms for chaotic systems* (Springer-Verlag, 1989).
- [18] S. Wolfram, *Theory and applications of cellular automata*, Advanced Series on Complex Systems (Singapore: World Scientific Publication, 1986).
- [19] G. H. Golub and C. F. van Loan, *Matrix computations* (The Johns Hopkins University Press, 1996).
- [20] W. H. Press, S. A. Teukolsky, W. T. Vetterling, and B. P.

- Flannery, *Numerical recipes in C* (Cambridge University Press, 1992).
- [21] K. Kaneko, Prog. Theor. Phys. Suppl. **99**, 263 (1989).
- [22] P. Manneville, in *Macroscopic modelling of turbulent flows* (Springer Berlin / Heidelberg, 1985), vol. 230 of *Lecture notes in physics*, pp. 319–326.
- [23] L. Keefe, Phys. Lett. A **140**, 317 (1989).
- [24] L. Junge and U. Parlitz, Phys. Rev. E **61**, 3736 (2000).
- [25] H. Yang, K. A. Takeuchi, F. Ginelli, H. Chaté, and G. Radons, *Hyperbolicity and the effective dimension of spatially-extended dissipative systems*, arXiv:0807.5073 (2008).
- [26] J.-P. Eckmann and D. Ruelle, Rev. Mod. Phys. **57**, 617 (1985).
- [27] K. Geist, U. Parlitz, and W. Lauterborn, Prog. Theor. Phys. **83**, 875 (1990).
- [28] C. Skokos, *The Lyapunov characteristic exponents and their computation*, arXiv:0811.0882 (2008).